Journal of Marine Science and Engineering

MDPI

Review

Flow, Sediment, and Morpho-Dynamics of River Confluence in Tidal and Non-Tidal Environments

Ahmed Bilal [1,†], Qiancheng Xie [2,*,†] and Yanyan Zhai [3,*,†]

[1] College of Water Conservancy and Hydropower Engineering, Hohai University (HHU), Nanjing 210098, China; ahmed.bilal@hhu.edu.cn
[2] Division of Fluid and Experimental Mechanics, Luleå University of Technology (LTU), 97187 Luleå, Sweden
[3] Division of Fluid Mechanics, Coastal and Maritime Engineering, Technical University of Denmark (DTU), 2800 Kgs, 2800 Lyngby, Denmark
* Correspondence:qiancheng.xie@ltu.se (Q.X.); yzhai@mek.dtu.dk (Y.Z.); Tel.: +46-7228-703-81 (Q.X.); +45-9145-8313 (Y.Z.)
† Co-first author: The authors contributed equally to this work.

Received: 9 July 2020; Accepted: 6 August 2020; Published: 7 August 2020

Abstract: River confluences are the key features of the drainage basins, as their hydrological, geomorphological, and ecological nature strongly influences the downstream river characteristics. The river reaches near the coastal zones, which also makes them under the influence of tidal currents in addition to their runoff. This causes a bi-directional flow and makes the study of confluences more interesting and complex in these areas. There is a reciprocal adjustment of flow, sediment, and morphology at a confluence, and its behaviors, differ greatly in tidal and non-tidal environments. Existing studies of the river junctions provide a good account of information about the hydrodynamics and bed morphology of the confluent areas, especially the unidirectional ones. The main factors which affect the flow field include the angle of confluence, flow-related ratios (velocity, discharge, and momentum) of the merging streams, and bed discordance. Hydraulically, six notable zones are identified for unidirectional confluences. However, for bi-directional (tidal) junctions, hydrodynamic zones always remain in transition but repeat in a cycle and make four different arrangements of flow features. This study discusses the hydrodynamics, sediment transport, morphological changes, and the factors affecting these processes and reviews the recent research about the confluences for these issues. All of these studies provide insights into the morpho-dynamics in tidal and non-tidal confluent areas.

Keywords: river confluence; morpho-dynamics; tidal effects; flow patterns; sediment transport

1. Introduction

River confluence is an essential geomorphological node that controls the downstream routing of flow and sediment. In light of its importance, there has been an increased recognition that more attention needs to be paid to the interaction of flow-sediment-morphology. The study of river confluence has seen significant advances mainly regarding their flow features, or the role of morpho-dynamics here, in influencing such features.

Much of the persisting research focuses on the morpho-dynamic evolution of a confluence and their interdependencies on the runoff river. Taylor [1], as a pioneer, worked on the flow characteristics of rectangular channels. Later, Miller [2] investigated, after various field surveys, the relationship between the width, depth, and cross-sectional area of tributaries and post confluence

channels for the hilly stream junctions. Mosley [3] discussed the asymptotic behavior of bed features concerning confluence angles and expanded the research topic more scientifically.

Best [4,5] suggested dividing different flow features within a confluence. Yuan, et al. [6] recapped the current level of knowledge and development achieved during studies of uni-directional open channel confluences. Dixon, et al. [7] and Umar, et al. [8] studied the river confluences using remote sensing imagery, a relatively new approach, to study the behaviors in the river reach scale. These studies reaffirm the strength of the hypothesis from Best [4], i.e., to segregate the identifiable confluent hydrodynamic patterns into six flow zones. Further, these works also examined such morphological features as lateral bars attached to banks, deep scour-holes, tributary-mouth bars, and a zone of sediment deposition.

In addition to the natural river confluences, junctions that are there in urban drainage and the irrigation canal systems are examples of confluences in the built infrastructure. Based on different flow and channel characteristics, river confluences are differentiated as those present in (i) upland reaches, (ii) middle reaches, which are represented in the majority of confluences studied so far, and (iii) the reaches near coastal areas, which are called tidal confluences. In terms of flow direction, the tidal confluences are distinct from non-tidal ones because they have a bi-directional continually varying flow, while the others only have a uni-directional flow.

This leads to a general confluence classification based on flow direction, as shown in Figure 1. The classification takes the majority of common confluences into account. However, there are some special confluences sharing characteristics of two or more categories shown in Figure 1. For instance, coastal confluences are not necessarily natural and can also be man-made; even for upstream river confluences, the flow direction is possibly reversed during compound surges from other rivers. These exceptional cases are not considered in the present work.

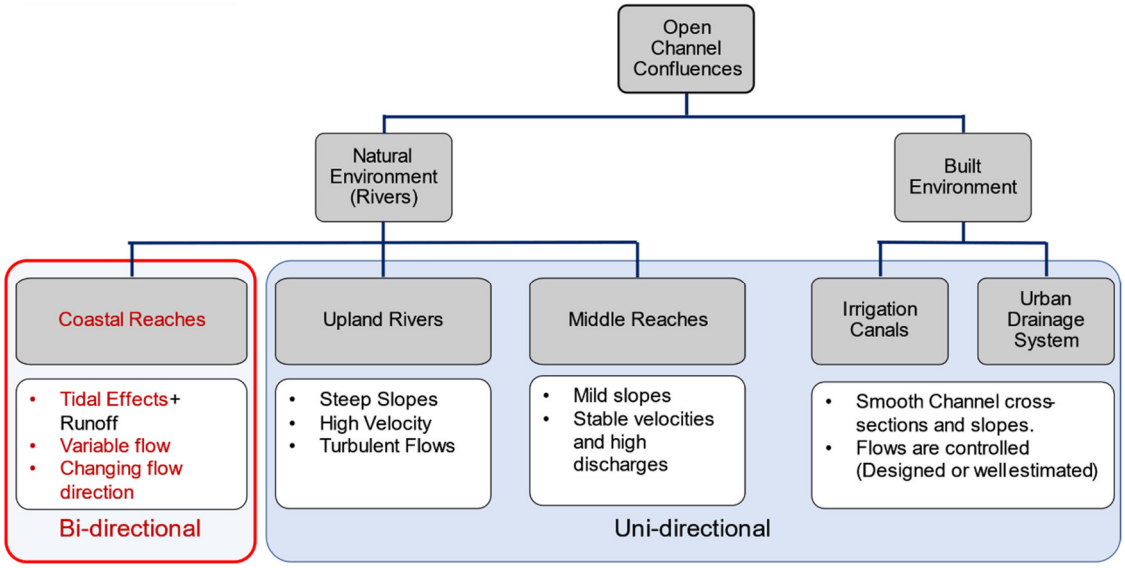

Figure 1. Confluences classification.

Based on the prevailing flow and sediment conditions, a river confluence can be subdivided into a non-tidal and tide-driven one (Table 1). For the former, reducing the river sediment input impacts the entire system dynamics. For the latter, the sediment is subject to both freshwater run-off and the dominating oceanic currents, showing a bidirectional transport feature driven by flood and ebb tides. The resulting morpho-dynamic adaption time in a non-tidal river is usually from months to years. In a tidal environment, there exist two different time scales: the first one is associated with the tidal period and the second one with the morphodynamic evolution. In a tidal period, sediment transport varies to adapt to the instantaneous tidal driven hydrodynamics. Still, if the system is not at equilibrium, although being very weak, a residual sediment transport may be present at the end of each tidal cycle. This latter contribution is responsible for morphological variation, which may be relevant in the long term [9,10].

Table 1. Comparison of the main characteristics between a tidal and non-tidal confluence.

Items	Non-Tidal Confluence	Tide-Driven Confluence
Flow volume timescale	daily/seasonal	hours
Main sediment forcing	river run-off (fresh-water)	tides (salty-water)
Sediment concentration timescale	days–weeks	hours
Sediment transport direction	unidirectional	bidirectional
Morphodynamic adaption time scale	months–years	weeks–months/years

At a confluence, the flow and sediment behaviors and the morphological changes are associated with its unique geometry. Figure 2 shows the definition of confluence geometry. Particularly, the confluence angle (θ) and the bed discordance are the typical geometric factors that affect the confluent morpho-dynamics. In Figure 2, the θ is defined as the angle between two tributaries, measured from upstream. Q (m^3/s) = flow discharge, V (m/s) = velocity, d (m) = water depth, W (m) = channel width, and h_d = elevation difference between the tributary and main channel. The subscripts "1" and "2" represent the tributaries 1 and 2, respectively.

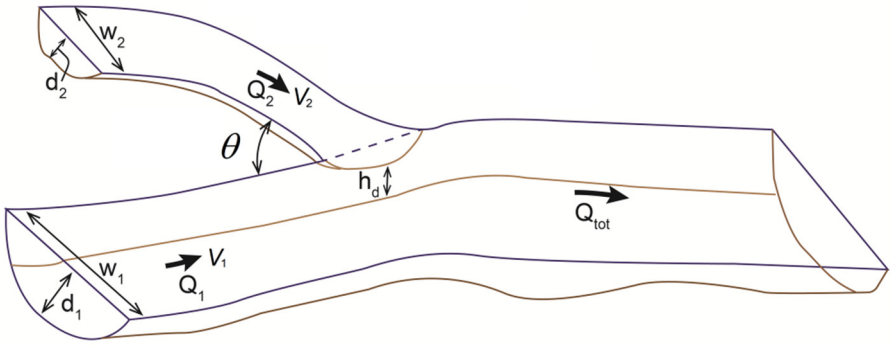

Figure 2. Definition of confluence geometry.

At a confluence, hydrodynamics, sediment transport processes, and channel morphology interplay and modify each other. The output of one process becomes the input for the other two. Each of the different processes adjusts itself and then gives a response or feedback to the system. This amalgamation is happening simultaneously. This continuous cycle of input–output evolves the system. Therefore, it is not reasonable that a river system is studied in isolation, especially for its long-term behavior. The interaction of the three main components affecting each other, is described by Leeder [11] (Figure 3a). This figure, however, is an oversimplification of a complex system. Ashworth and Ferguson [12] suggested a relatively detailed conceptual model for the interaction of different components (Figure 3b). Spatio-temporal variability of these components for a tidal confluence is even more complicated.

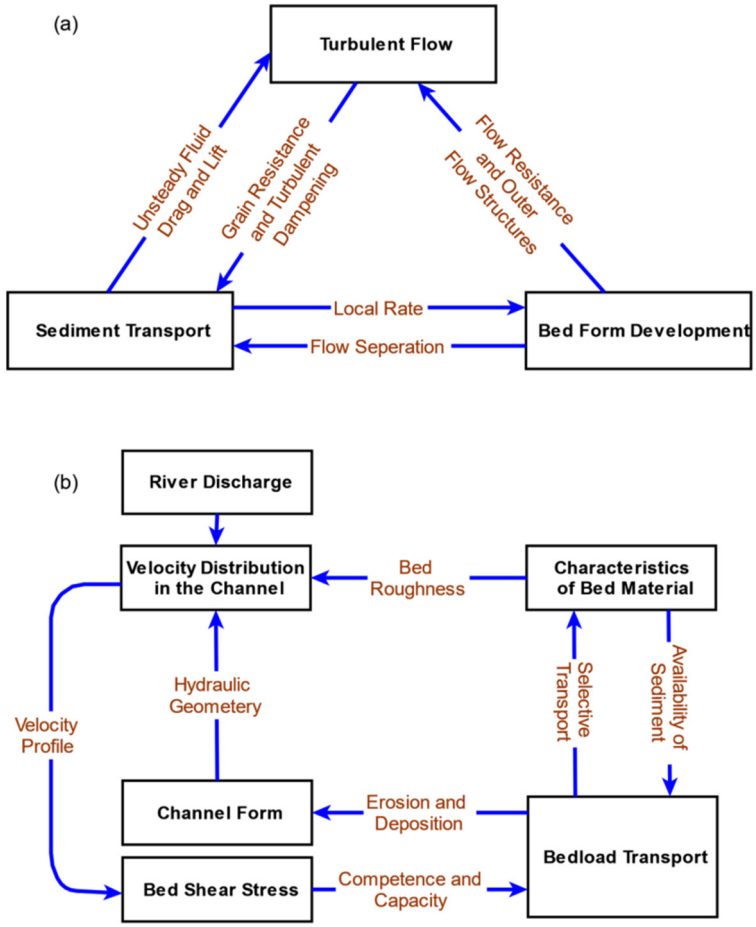

Figure 3. The conceptual relationship between flow, sediment, and morphology at a confluence, as proposed by (**a**) Leeder [11] and (**b**) Ashworth and Ferguson [12].

Both models emphasize that the hydrodynamics, the carried sediment, and the river morphology are interlinked. This interaction is a never-ending cycle of taking feedback from each other, modifying themselves, and then this modification becoming feedback for other processes. Both of these conceptual models are physically combined, as shown in Figure 4.

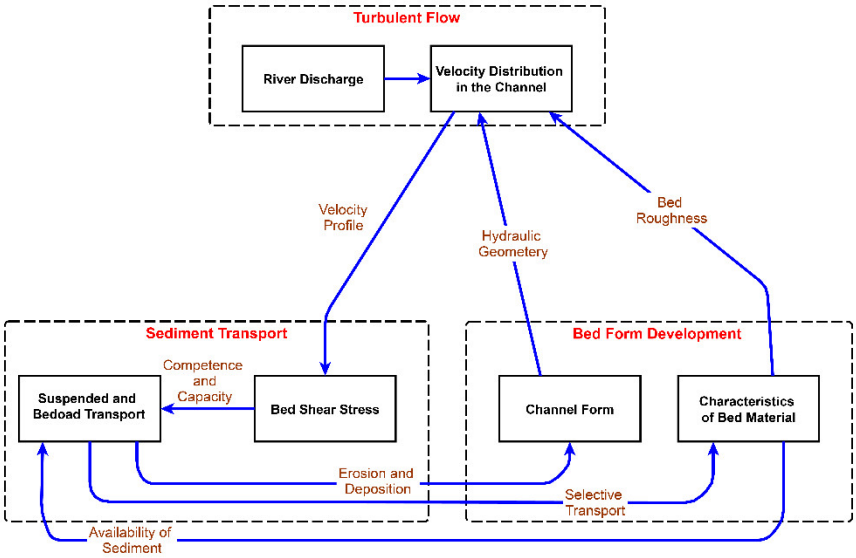

Figure 4. Unification of conceptual models by Leeder [11] and Ashworth and Ferguson [12].

Tidal confluences experience simultaneous flow variability, both in magnitudes and directions. Therefore, its flow structure and feature of erosion and deposition are different from those of a non-tidal one. Furthermore, if such a confluence is near an urban area, awareness about the flow and morphological changes will be of practical concern. For example, precautionary measures for infrastructure development around or in such confluences will be more realistic. Bolla Pittaluga et al. [13] worked on the morphological equilibrium of many tidal configurations using a 1D model. Xie, et al. [14] examined the morpho-dynamics of a tidal confluence through field investigations and numerical simulations. Zhou, et al. [15] reviewed the concept of equilibrium and suggested that it can only be found in ideal situations of numerical or physical models. They discussed that since a tidal river undergoes a constant variability of environmental and anthropogenic factors, equilibrium in such an environment is far from reality. Wolfram, et al. [16] and Gleichauf et al. [17] analyzed the intra-junction flow dispersion at a well-mixed tidal river junction in Sacramento-San Joaquin Delta (USA). A few studies on tidal confluences include the work investigating scour-hole evolution [18–20]. Ferrarin, et al. [21] identified the hole's geomorphological characteristics in tidal rivers and compared them with the ones in the non-tidal environment.

Field investigations [5,21,22], laboratory experiments [6,23–25], and numerical simulations [14,26–30], complementing each other, are common methods to help understand the morpho-dynamics of a confluence. Bradbrook [31] suggested that combining all three methods would help to understand the confluences more comprehensively. Based on the available literature regarding the confluences in tidal and non-tidal environments, this paper reviews their flow features, sediment transportation, morphological characteristics, and their interactions.

2. Hydrodynamics of River Confluences

At a confluence, the classical viewpoint of flow features is the definition of six identifiable flow zones. Best [4,32] firstly proposed the conventional model, which includes a region of (i) flow stagnation, (ii) flow deflection, (iii) flow separation, (iv) maximum velocity, (v) gradual flow recovery, and (vi) two shear layers (Figure 5). Best [4] mainly discussed these zones on a two-dimensional scale, i.e., a depth-averaged scenario. Each zone's actual size depends on such factors as tributary flow ratio, confluent angle, bed discordance, upstream planform, etc.

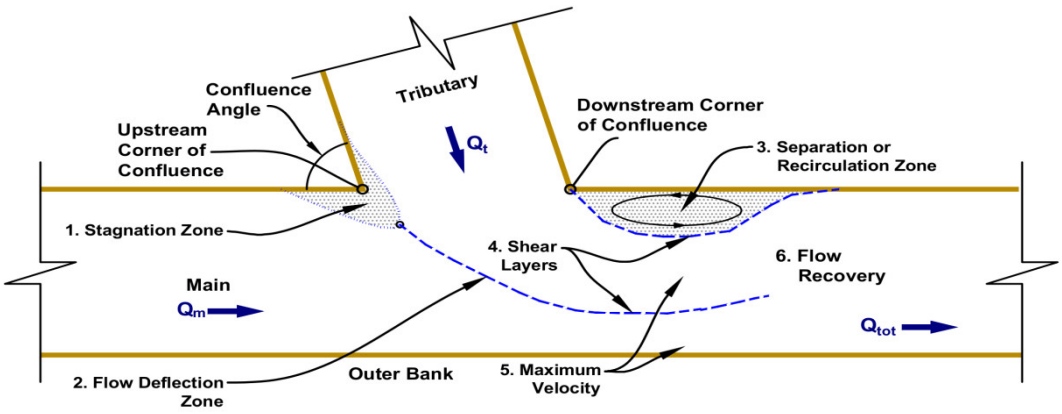

Figure 5. Six identifiable flow zones at a confluence—adapted from Best [32].

2.1. Mixing Zone and Shear Layer

Initial research on confluences deals mostly with the mixing of flows [33]. The mixing often leads to a downstream shear layer, which enhances turbulent mixing. In terms of driving the mixing process in confluences, four main processes are identified: the quasi-2D vortices, helical secondary circulation cells, the bed discordance, and mass transfer [23,34–39]. To meet the requirements of mass conservation, there exists a transfer from the faster, decelerating flow to a slower, accelerating flow [40]. Mixing in the confluent area is also influenced by the secondary flow structures observed with cells of clockwise rotation [41].

The mixing interface position sometimes is visible through the turbidity of the water or is observed indirectly by using proxy approaches. These include using the electronic conductivity [42], differences in the chemical isotope composition [43], or, as in the Kaskaskia River—Copper Slough confluence, by identification of temperature differences between the two tributaries [44]. These methods may be used to capture the change in the mixing layer position over time.

The "shear layer" is considered as the major zone of a junction, where there is a significant velocity gradient between the two flows (Figure 5). It extends for a substantial distance downstream, from the flow stagnation zone to the flow recovery zone [45]. The shear layer is considered as strongly turbulent, featuring high shear stresses and well-defined coherent flow structures such as Kelvin-Helmholtz instabilities [46]. The existence of a shear layer indicates that the flows of different velocities are running parallel to each other, encouraging the development of Kelvin–Helmholtz instabilities, which can pair up, split, or merge as they move downstream [34]. This results in an enhanced exchange of momentum and mass (e.g., sediment and pollutants) across the shear layer [6].

The shear layer encourages Kelvin–Helmholtz instabilities thereby leading to the eddy generation. However, for a given large θ and a comparable velocity, instead of generating eddies there, Kelvin–Helmholtz instabilities develop on either side of the stagnation zone. As these eddies come from either side of the stagnation zone, they rotate in opposite directions and then merge in the mixing zone [27]. These findings match the observations of wake-generated coherent flow structures around the stagnation zone [47]. Regarding this particular feature, more studies are required to consolidate it. Further research is desirable to determine how dependent this is on the confluence bathymetry, geometry, momentum ratio, and other factors.

2.2. Flow Stagnation

The stagnation zone, as shown in Figure 5, is known as an area of recirculating flow at the upstream junction corner [48,49]. It acts as an obstacle to enhancing the development of wake-generated shear flows around it [27,48,49]. However, it is still not clear how widespread these zones are in natural confluences, what triggers them to form, and whether these causes are associated with the type of confluence.

Rhoads and Kenworthy [48] proposed that it is the low velocity near the tributary banks, which is the cause of the development of this zone. An alternative explanation is that superelevation in the mixing zone or in the stagnation zone itself results in a negative pressure gradient towards the upstream corner, which encourages the lower or negative velocities [50,51]. However, the understanding of the stagnation zone remains still incomplete until more stagnation zones are investigated for their prevalence and mechanics.

2.3. Flow Separation

The flow separation zone, in Figure 5, is an area of lower pressure and flow recirculation at the downstream corner. The zone is known to increase in size with larger θ and higher tributary discharges [52]. From 3D numerical experiments, Huang, et al. [53] identified that the zone of flow separation expands substantially from its minimal at 30° to an angle of 90°. They suggested that the θ increase causes an increased conversion of lateral flow momentum into downstream channel flow momentum. This conversion increases the loss of kinetic energy, which then results in the expansion of the zone and deepening of water surface depression.

Ashmore et al. [22] discussed that in reality, natural confluences have partial or no zone of flow separation due to their banks changing direction more gradually than in simplified flume experiments. Although later field studies support the existence of flow separation zones [54], as yet, it is not clear if the causes proposed by Huang, et al. [53] apply to natural confluences.

In the case of discordant confluences, where there exists a bed level difference between two tributaries, it is found that flow separation on the downstream corner is minimal [55–57]. Studies on flume experiments [58] also confirmed that a concordant confluence has a small flow separation zone that is not present in a similar, discordant case. Biron, et al. [51] found superelevation at the

downstream corner of the discordant Bayonne-Berthier confluence and suggested that the upwelling of flow from the main channel disrupts the formation of a flow separation zone. Its causes may also include the erosion of the downstream corner, in the case of curving banks or the presence of a bar on the downstream corner, disrupting the flow separation [55,57]. In a way, the presence of flow separation is related to many factors, including channel planform, bathymetry, and the interplay of tributaries flow, etc.

2.4. Flow Acceleration and Recovery

The flow acceleration zone is believed to exist due to the constriction of two tributary flows into a smaller total cross-sectional area. Indeed, the early research by Best and Reid [52] found that flow separation zones assist this acceleration by constricting the flow, with near-bed velocities at a 90° confluence up to 1.3 times larger than those at a 15°. Flow acceleration will increase the bed shear stresses and has, therefore, been highlighted as a potential contributing factor to the development or maintenance of scour-holes [59]. The principle of continuity requires that a decrease in channel cross-sectional area results in flow acceleration in the downstream channel. However, the complexity of natural river confluence morphologies means that the flow acceleration zone is not always clearly present or consistent in its form [22,60,61].

Evidence also shows that the stream entering the confluence with the larger velocity gradually widens its share of the common channel width at the expense of the slower stream [40]. It is believed that there is a dynamic adjustment between two streams past their confluence [62]. The faster stream slows down and, to conserve flowrate, expands laterally, thus squeezing the slower stream, which accelerates, to retain its flowrate. Thus, the faster stream decelerates, while the slower stream accelerates, and the line demarcating the two streams migrates laterally toward the side of the lower velocity. Further downstream, the flow convergence pattern diminishes, indicating that the flows become aligned with each other; and also, with the adjustment of the two flows, secondary flows disappear, and a cross-sectional equilibrium is achieved.

2.5. Tidal Flow Pattens

In tidal environments, in addition to the run-off, the confluence is also affected by tides. The shift of the dominant processes between run-off and tides featuring periodical changes in both magnitude and direction induces more degrees of complexity in terms of flow patterns. As a result, the flow patterns in terms of the conventional flow zone definitions are different. Unlike unidirectional confluences, there are limited references available regarding the tidal confluence flow patterns, and its complexity has not drawn much attention [14,18,28].

A recent study performed 3D simulations for a tidal confluence in China [28] to examine the surface flow features based on extensive field measurements. It is noticed that the typical confluent flow patterns change more gradually and repeat in a cycle with the progression of a tidal phase. Therefore, it proposed four noticeable arrangements of hydraulic features and asserted that hydrodynamics of a tidal confluence remain in transition between these four states. These four flow scenarios with respect to the discharge conditions are shown in Figure 6. Figure 7 illustrates the four corresponding flow patterns during a full tidal cycle, i.e., the maximum flood tide, flood to ebb transition, the maximum ebb tide, and finally, ebb to flood transition [28].

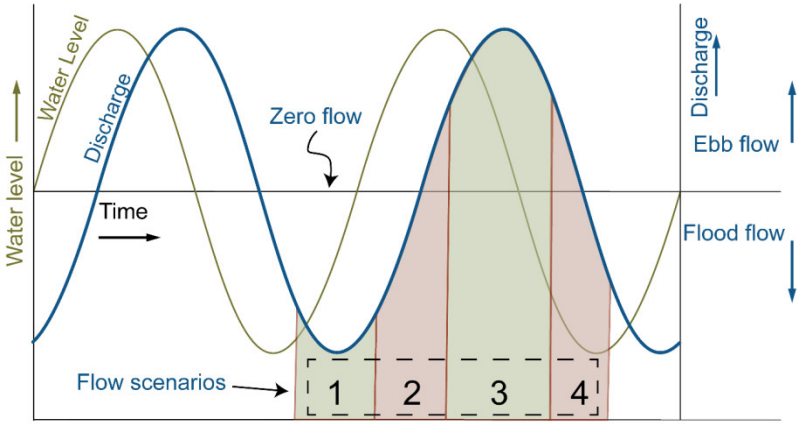

Figure 6. Schematic of flow scenarios used for studying the hydrodynamics of tidal confluences.

Figure 7a corresponds to the hydraulic condition when the discharge near the confluence is at its lower peak. This means that the flow is running from downstream to upstream, and hence, the intersection acts as a bifurcation. A clockwise recirculating eddy appearing on the angled tributary is noticed here. The location of this zone of recirculation, as well as its direction of rotation, change during the next three scenarios (Figures 7b–d). During the peak of the positive flow (Figure 7c) in the main channel after the confluence, the flow behavior resembles that of unidirectional confluences. The hydrodynamics during the transition from positive (ebb) to negative (flood) flow is captured in Figure 7d.

In addition to the tidal flow features, the study captures some interesting observations regarding the hydraulic behavior of the tidal confluence. The most observable behavior of the transition cases is that the change of flow direction in both tributaries does not occur at the same time due to their geometric and hydraulic asymmetry [28]. This non-coherent flow reversal results in a "no slack water" condition at tidal channel intersections.

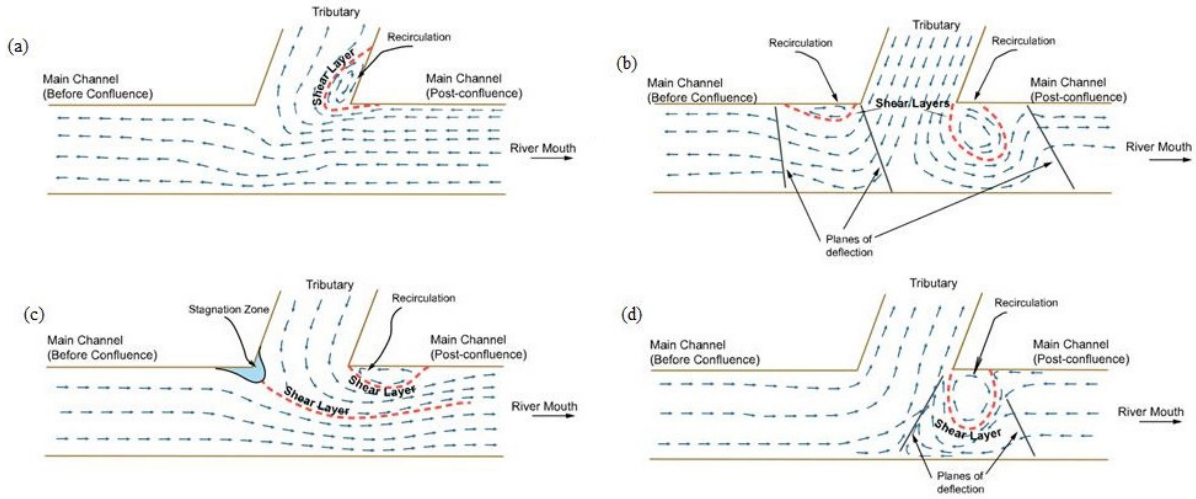

Figure 7. Schematic flow patterns of tidal confluence: (**a**) the maximum flood; (**b**) flood to ebb transition; (**c**) the maximum ebb; and (**d**) ebb to flood transition.

In a confluence dominated by tides, Xie, et al. [14] also investigated the interaction of runoff and tides. While for the flood tide, the run-off and the tide are in the opposite direction, thus offsetting each other. Apart from the water levels, the confluence flow at the maximum flood tide differs in both flow direction and magnitude from that at the maximum ebb tide, which depends on the tidal flow direction. At the ebb tide, a zone of flow separation also exists close to the left river

bank. The prevalence holds that the velocity of the ebb tide is higher than that of the flood tide that is attributed to the addition of runoff and tide.

3. Sediment Transport and Morphology

3.1. Sediment Transport

Many studies have looked into the sediment dynamics of river confluences on a catchment scale. Some of these have looked at the impact of sediment influxes from tributaries into the confluence and have found that it interrupts the general process of downstream fining in the main channel [61,63–67]. The conclusion obtained by Rice [65] is based on an extensive investigation of over 100 confluences. Benda et al. [68] suggested that the main tributary has a higher chance of causing a sediment discontinuity in the main channel. However, Unde and Dhakal [54] argued that since the grain size for very large tributaries is likely to be similar in both channels, the effect of the tributary sediment input may be reduced. Other artificial factors that have been highlighted for their impacts on the confluence sediment transport include the construction of dams, sluice gates, bridges, and other additional restrictions of flow and sediment upstream [68–70]. The sediment influxes also affect the morphology of the confluence, with large debris fans capable of rerouting the main channel, while significant sediment inputs change the main channel slope [64,68,69]. The slope tends to decrease upstream of a massive sediment influx from a tributary, with a corresponding increase downstream [69].

At a river confluence, in addition to examining the sediment dynamics directly, other theories and hypotheses such as the flow field, the bed shear stress, and stream power theory, etc. also help to understand the sediment mechanics [55]. Several studies have highlighted the role played by turbulence in bedload transport. The turbulent structures generated in the mixing zone are considered to be crucial for potential entrainment and transportation of particles [32,57,71]. However, Boyer, et al. [46] investigated research in the Bayonne-Berthier confluence and found that the maximum bedload transport values are at the edge of the shear layer, rather than in the zone of maximum turbulence. This suggests that the link between strong turbulence and bedload transport may not always be straightforward. In particular, it is noted how the mean velocity and Reynolds shear stress does not accurately explain bedload transport, with variations in the instantaneous values considered more important [71].

Many researchers link the bed shear stress with sediment movement, although this may not always be a reliable indicator of sediment motion [51,72]. Szupiany et al. [60] observed for the Rio Parana confluences that the suspended load transport does not correlate well with bed shear stress but occurs in narrow zones linked to the flow field, the upstream sources of sediment, and in some cases, topographic steering. Assuming that there is a link, Bradbrook, et al. [73] suggested from their CFD results that, under the right circumstances, confluences with a small difference in bed elevation experience sufficient bed shear stress to cause erosion that deepens the tributary step. However, as yet, no studies have followed this up and tested the hypothesis.

In tidal confluences, the amount of bedload is often negligibly small, meaning that the sediment is mainly in suspension with the water, a common feature of many fluvial rivers [74]. The suspended sediment concentration is dependent on the flow discharge, showing an hourly variation. The sediment dynamics are closely linked to the confluent flow dynamics described above. As aforementioned, the cohesive sediment of mud (silt and clay) has completely different dynamics than non-cohesive sediment, consisting of sand. In a tidal environment, cohesive sediment movement is somehow affected by the flocculation, leading to a lower settling velocity [75]. The difference arises from the electrochemical interactions of clay and silt particles, so the cohesiveness of sediment depends on their contents and also the salty water concentration. Laboratory experiments show that sediments become cohesive when the clay and silt contents are over 3%–5% [76].

Interplaying with the freshwater flow, tides penetrating the river lose energy in the bottom boundary layer; this energy dissipation is transformed into bed shear stress (τ_b) [77]. In most

studies dealing with the cohesive sediments, bed erosion and deposition are linked to critical shear stresses for erosion ($\tau_{cr,e}$) and deposition ($\tau_{cr,d}$), separately. When $\tau_b < \tau_{cr,d}$, the deposition takes place; while if $\tau_b > \tau_{cr,e}$, erosion occurs. The bottom composition determines the critical shear stress, and cohesiveness augments the critical value by 2–5 times [76] as compared to non-cohesive sediment. This implies that the flow to erode the bed layer with the tidal effect should have more momentum, although the sediment is finer, which is not in line with the findings for the non-tidal river regarding the fine sediment transport.

During flood tide, it is common to observe sediment in a high concentration transporting landward. The sediment deposits easily during the flow reversal, i.e., the shift between flood and ebb tides. A certain amount of particles consolidates and is not re-suspended during the ebb tide [64]. This is the main sediment transport pattern for rivers driven by strong tides. This transport scenario may become the opposite in stormy periods, becoming ebb dominated. For non-tidal rivers during the wet season, the peak freshwater flow with a high sediment concentration may govern the sediment transport in the river [26,78,79]. Some exceptions are subject to the availability of sediment sources.

All of these studies provide insights into the sediment dynamics in tidal and non-tidal confluences. To comprehensively figure out their sediment transport processes is still challenging in the field of geomorphology, especially for the tidal cases. It is advisable to see extensive field measurement data and theoretical progress as foundations to help in understanding the sediment dynamics.

3.2. Morphological Characteristics

3.2.1. Scour-Hole

In a confluence, scour-hole is a common bathymetry feature, shown in Figure 8 as an example. The research was pioneered by Mosley in discussing its morphological features and changes [3]. He found that there is a possibility of scour-hole existence with large θ, strong turbulence, and identical discharges. While Wallis et al. [61] investigated eight confluences and found that scour-hole exists in only five out of those. Bed discordance is regarded as one factor leading to the absence or size reduction in scour-holes [55,58]. It is yet not very clear how the flow behavior and sediment dynamics influence the scour-hole features. This ambiguity in the links between the scour-hole and sediment movement may explain why these are not universal features of river confluences.

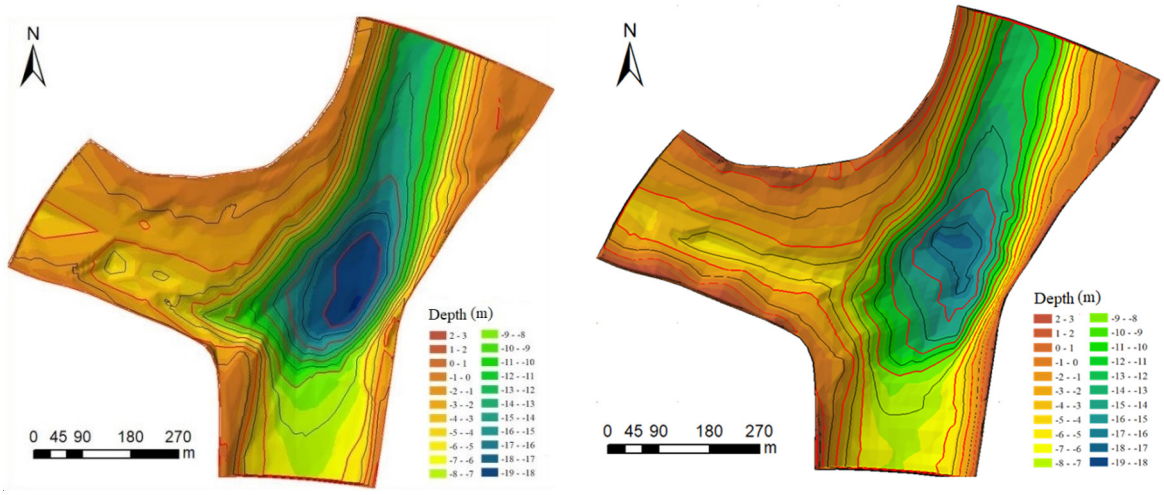

(**a**) (**b**)

Figure 8. Measured bathymetry of a tidal confluence: (**a**) 2010; (**b**) 2015 (adapted from Xie [80]).

The generation and maintenance of scour-hole encourage much debate in the river confluence research. Many hypotheses have been proposed for the generation of the scour-hole, such as the large flow velocity, strong turbulence, the effect of the shear layer, or the curvature-induced helical circulation [5,59,81–84]. Yuan et al. [6] found that the downwelling flow and upwelling flow involved in helical motions, associated with the intense shear to the bed, are responsible for sediment entrainment and scouring, thereby generating the scour-hole. Rhoads et al. [59] noted that helical flow, shear layer turbulence, and flow acceleration help to maintain the shape of scour-hole by ensuring that it is an area of high bed shear stress. Constantinescu et al. [27] argued that it is helical cells that are most significant to maintain the scour, although they conceded that this could change if the mixing zone produces Kelvin–Helmholtz instabilities.

From the point view of sediment dynamics, it is also speculated that particles from each tributary are routed around the scour-hole, leading to the maintenance of the scour-hole and a zone of maximum sediment transport at its downstream [5,85]. However, Roy and Bergeron [86] found that particles, regardless of size, could travel through the scour-hole, with particles from both tributaries capable of doing so depending on the flow discharge. Based on the investigation of the Bayonne-Berthier confluence, Boyer et al. [46] argued that the link between strong shear layer turbulence and maintenance of the scour-hole might not be as straightforward as the classical model suggests. In a way, their findings verify that the highest suspended sediment concentration is in the vicinity of the scour-hole. At a given confluence geometry, the likelihood is that all three factors, i.e., turbulence, secondary flow in the form of helical cells, and sediment routing, are linked to each other and affect the scour-hole [87].

Research has also examined the evolution of scour-hole over longer timespans. Scour-hole can rotate, evolve through lateral and streamwise migration, or change in size, with respect to the variation of flow and sediment [85]. In light of the scour-hole infilling, Best and Rhoads [23] hypothesized that, on a larger scale, the migration of tributary bars into the junction dominates the scour-hole infill. There is a tendency for scour-hole development on the braiding planform during flows with a higher magnitude than average; similarly, massive floods will also cause noticeable changes to the planform [88]. If a braid plain is more susceptible to avulsion, then scour-hole would be reworked more frequently, while sediments are less likely to be stored for long periods [89].

In a tidal environment, the alluvial process in terms of scour-hole erosion and deposition is different. Xie et al. [14] and Xie [80] investigated, through the field and numerical studies, the alluvial behaviors of a scour-hole dominated by strong tides (Figure 8). They found that the shifting tidal directions induce the scour-hole migrates in both directions that do not exist in unidirectional run-off flows. The flood tides govern its sediment transport and play a dominant role in the scour-hole deposition, while the ebb tides with run-offs lead to erosion. Ferrarin et al. [21] identified 29 scour-holes by examining their geomorphological characteristics and comparing them with scours in non-tidal ones. It was demonstrated that the maximum depth of the scours is positively correlated with the tidal prism of the channels joining the confluence. As a consequence of changes in the flow regime, their findings also preliminarily revealed, in a century-scale, the morphological dynamics of scouring.

So far, the collective effect of different factors on the confluence morphology has not been well developed. However, there are studies available that empirically state the impact of one particular factor on the morphological changes. For example, Ferrarin et al. [21] and many other studies [90,91] linked the relative scour depth (H_r) with the θ and found that they are positively correlated. The H_r is the ratio of the mean upstream channel depth (H_m) to scour depth (H_{sc}).

$$H_r = \frac{H_m}{H_{sc}} \quad (1)$$

$$H_m = \frac{\sum_1^n H_n}{n} \quad (2)$$

where H_n is the mean water depth of the n^{th} channel, and n is the number of tributaries. Ferrarin et al. [21] noticed that some confluences have three and even more tributaries. Figure 9 shows the relationship between H_r and θ both in tidal and non-tidal confluences. Since many other factors also

play their roles, it indicates a 35% dependence ($R^2 = 0.35$) of H_r on the θ.

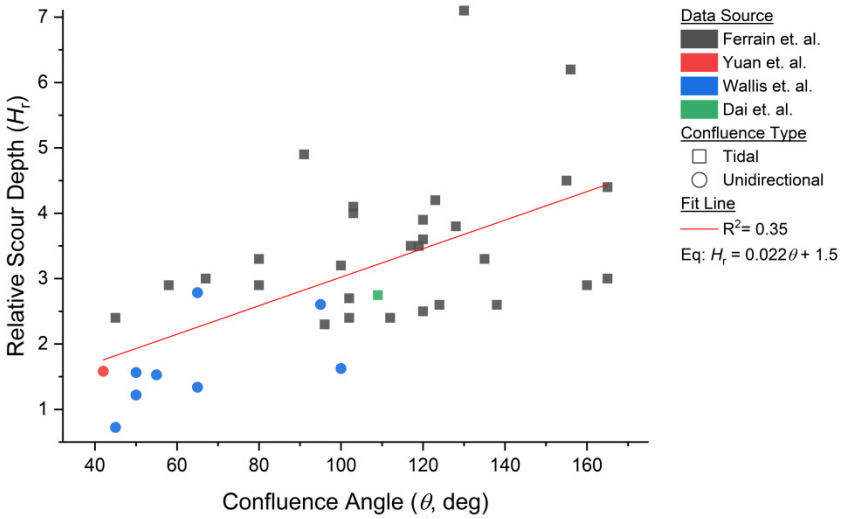

Figure 9. Relationship between H_r and θ. The data source is from studies carried out by Ferrarin et al. [21], Yuan et al. [6], Wallis et al. [61], and Dai et al. [28].

In view of the tidal scour-hole formation, maintenance and evolution need to be further investigated based on the knowledge available on non-tidal ones.

3.2.2. Mid-Channel Bars

Mosley [3] also identified the potential for mid-channel bars to emerge in high angle ($\theta > 60°$) confluences, finding that higher bed elevations and transport rates either side of the scour-hole joined downstream into an area of deposition. It is the combination of scour-hole erosion and sediment routing around it, which favors the deposition [32] and sediment accumulation slightly downstream of the area of maximum bedload transport [85].

A study by Orfeo et al. [92] noticed that for a confluence–diffluence unit on the Rio Parana, the flow starts to diverge at a position at a significant distance upstream from the front of the mid-channel bar. Once a mid-channel bar is in place, the flow field would appear to be conducive to the further deposition of sediment on the front of the bar, thereby encouraging growth. However, for sediments to accumulate in the first place, there must be some initial cause of flow divergence or an alternative process that reduces the downstream flow velocities and encourages sediment deposition. As such, confluence symmetry is believed to be an important factor in determining whether a mid-channel bar will form, due to its impact on flow divergence downstream of the scour-hole [36].

3.2.3. Bank-Attached Bars

There has been limited research into the development of bank-attached bars in river confluences in both the flow stagnation and separation zones [5]. The flow separation zone is known to be an area of lower pressure and recirculating flow, which encourages sediment deposition [83]. The same is true for the lower velocities in the flow stagnation zone at the upstream corner of many confluences.

Parsons et al. [36] suggested that lateral bars are more common features on the asymmetric confluences where there is a flow separation at the downstream corners. A confluence is described as a symmetric one if it has a planform that resembles a ”Y” shape; i.e., the centerline of the post-confluence channel bisects the θ in halves [32]. Otherwise, it is regarded as an asymmetric one. However, it is still not clear how often such bars are present at asymmetric confluences and how they evolve with changes in the flow conditions.

4. Key Factors Affecting the Morpho-Dynamics

4.1. Confluence Planform

In terms of the confluence planform, it has symmetric and asymmetric ones, and the major difference is the merging θ of the tributary flows to the post-confluence flow. For the former, both tributary-flows meet and run to align with the downstream flow direction; for the latter, one tributary flow is forced to turn through a much greater θ than the other. The asymmetry planform encourages a stronger helical circulation cell to develop in its tributary [78], instead of occurring in the confluence [44]. The results from the numerical modeling of both laboratory and natural confluences by Bradbrook et al. [93] and Bradbrook et al. [94] supported this view, with the back-to-back helical cell structure thought to become less representative of the flow field as asymmetry increases.

The planform, with respect to the θ, is an important factor in the strength of secondary flow. Mosley [3] suggested that a large θ enhances the turbulence—a result of the deflected flows from each tributary having a more intensive mixture. Results from the numerical modeling by Bradbrook et al. [56] supported this hypothesis, indicating that secondary flow circulation is much stronger for a confluence with $\theta = 30°$ compared to one with $\theta = 0°$. Ashmore and Parker [78] described this effect as a decrease in curvature radius, where a higher θ causes the flows of the two tributaries to pass through with enhanced turbulence. Penna et al. found that the maximum streamwise flow velocity does not necessarily increase with the θ, and it does not always occur in the contraction zone [95]. This fact is ascribed to the acceleration induced by the lateral flow that approaches the post-confluence channel. Furthermore, it is also evidenced that the higher the θ, the more extended the retardation zone and the lower the velocities in this region [95].

Symmetric or asymmetric planforms have a significant effect on both the hydrodynamic and morphodynamic features [96]. Parsons et al. [36] suggested that confluence symmetry is the key factor in the development of mid-channel bars. An example of this is the approximately symmetrical Mula-Kas confluence, where a partly vegetated mid-channel bar has developed [54]. At an asymmetric junction, Mosley [3] found that the scour-hole resides on a line that bisects the θ; erosion occurs on the bank opposite the tributary and deposition occurs at the downstream corner of the tributary. This encourages the development of a lateral bar on the corner, rather than the mid-channel bars that tend to develop at symmetric confluences [32,36]. The combined processes encourage the lateral migration of the downstream channel, ultimately resulting in the evolution of a symmetrical confluence planform [23,97].

Laboratory experiments of Mosley [3] confirmed that an increase in θ bolsters the depth and cross-sectional area of the scour-hole. In some confluences with smaller θ, e.g., less than 15°, there may not be an obvious scour-hole [5]. The augmentation in scour-hole depth with increasing θ is considered to be non-linear [23]; the most considerable growth in scour depth is expected as the θ comes close to 90° [3]. A possible explanation is that the greater routing of sediment around the scour-hole at higher θ supports its larger size to be maintained [5]. There is also evidence that the θ influences the position and shape of the scour-hole. Best and Rhoads [23] noted that the thalweg of a scour-hole tends to be positioned on a line bisecting the θ, and Ashmore and Parker [78] found that scour-holes move from trough to basin shapes at larger θ. The θ is, therefore, an important planform factor in determining the confluence morphology.

It may be noted that the effect of confluence planform on its morpho-dynamics cannot be treated in isolation. Evaluation of a junction—symmetric or asymmetric—also depends on other governing factors, such as the ratio of discharge, velocity, momentum, etc.

4.2. Ratio of Velocity, Discharge, and Momentum

At a confluence, it is common that one tributary is dominated by the other one due to the difference in flow input, resulting in unidentical morpho-dynamics features. To illustrate the behavior, velocity ratio V_r [62], the discharge ratio Q_r [82], and the momentum ratio M_r [98] are defined, given by:

$$V_r = \frac{V_1}{V_2} \quad (3)$$

$$Q_r = \frac{Q_1}{Q_2} \quad (4)$$

$$M_r = \frac{\rho_1 Q_1 V_1}{\rho_2 Q_2 V_2} \quad (5)$$

where, ρ (kg/m^3) = water density. The subscript 'r' represents the ratio.

In a confluence, a large ratio of two tributary velocities (i.e., where the V_r is much higher or much less than 1) highly affects the flow field compared with the θ, especially when $\theta > 30°$ [56,78]. However, with a smaller θ, this does not seem to hold valid. Bradbrook et al. [73] found very little cross-stream flow at parallel confluences, even when there are large differences in flow velocity between the tributaries. Therefore, the extent to which the V_r affects the flow field depends on the confluence planform.

The Q_r of two tributaries is also considered to play an important role in determining the location and strength of secondary circulations [27,73], as well as the mixing layer position [44] and its associated zone with higher turbulence and shear stress [98]. The Q_r is regarded to boost the migration of flow structures in river confluences. Rhoads and Kenworthy [44] discussed the variation of the mixing layer position at the Kaskaskia River—Copper Slough confluence subjected to different Q_r.

Research has highlighted the potential role played by the timing of the flood peaks from the tributaries. If the tributary flood peak arrives first, then bars can form at the tributary mouth [70]. On the other hand, when the flow peaks in the main channel, there can be a backwater effect in the tributary, with this slack water being an ideal place for the deposition of fine sediments [54,69,70,99]. These tributary mouth bars may also be affected by the Q_r, with the bar expected to migrate into the main channel, or to retreat in line with the main channel bank, depending on the M_r [57]. This migration could then have a similar effect on the nature of the scour-hole downstream [46]. Variations in the Q_r also have an impact on the position of the scour-hole. When the discharge of one channel dominates, the scour-hole is expected to migrate to align with the dominant channel [32,78]. It is evident from these results that the Q_r is significant not only for shaping the flow hydrodynamics [100] but also influences the sediment delivery and morphology [41].

In addition to the V_r and Q_r, the M_r is also considered important during the discussion about the hydraulics of the confluent zones. For instance, its effect should be taken into account when assessing the formation, duration, and strength of helical cells [27]. Examples of this effect are discussed in the research by Rhoads and Kenworthy [44] for the confluence of the Kaskaskia River formed by joining of its tributary stream—Copper Slough. They found that when dominant, the flow from Copper Slough causes a single, strong helical cell on the tributary side (much like in a meander bend). In contrast, the dominant Kaskaskia River gives only a weak convergence at the surface of the mixing interface [44]. A high momentum ratio pushes the mixing interface towards the right bank [44,100], especially at low flow. Meanwhile, with a low M_r, the mixing interface moves closer to the center.

4.3. Bed Discordance

When two tributaries have their bed elevations at a different level, it is called bed discordance (Figure 2). The bed discordance ratio D_r is defined as

$$D_r = \frac{h_d}{d_2} \quad (6)$$

The first investigations of bed discordance were performed on a parallel, discordant flume confluence by Best and Roy [34], with observations showing that the flow separates over the step, disrupting the mixing layer and causing far more rapid mixing in the shallow tributary.

Bed discordance has a significant impact on the confluence flow field, as shown in Figure 10. The shear layer, indicated by hatched shade, starts at the corner of the bed with higher elevation and gradually spreads vertically. A little far from the bed is a zone of upwelling, which is below the mixing layer, as shown in the gray shaded area [34]. Discordant confluences are considerably different from concordant ones, as shear layer distortion is considered more significant than the presence of scour-holes and helical cells [60]. The flow separation that occurs at discordant confluences distorts the vortices in the mixing layer [34,50,58,71], which encourages the faster mixing of the two flows, especially at low flows [42,50,57,101]. This increase in mixing speed at low flows may well be a function of the increased relative size of the step (compared to the water depth). Gaudet and Roy [101] argued that when river levels are shallow, water from the tributary with the higher bed elevation can flow over the water from the deeper tributary, causing a more rapid mixing of the two flows.

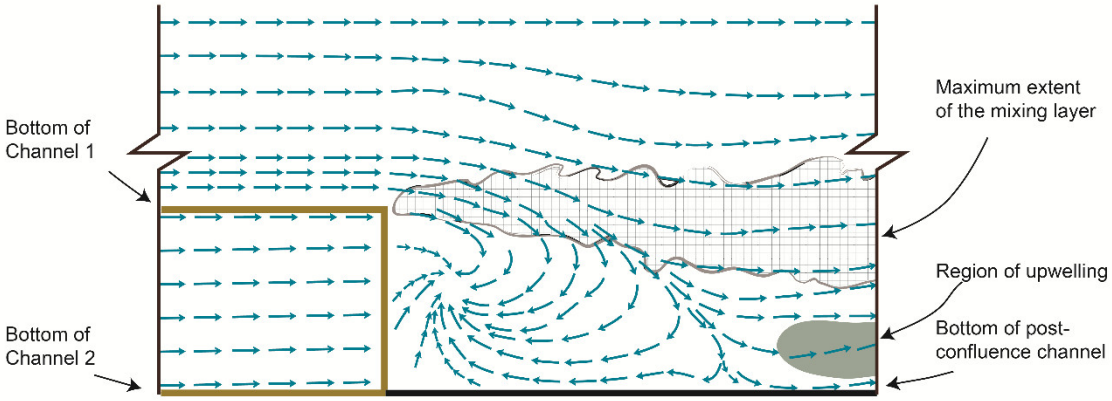

Figure 10. Flow fields at the bed of a discordant river confluence (Adapted from Best and Roy [34]).

It is suggested that bed discordance is commonly caused by the formation of tributary mouth bars [102], which have steep avalanche faces descending into the confluence scour-hole. Arguably the most important effect on the sediment dynamics and morphology is the tendency for a discordant bed to discourage the development of a scour-hole. With experiments on a 30° flume confluence, Biron et al. [58] found no evidence of helical cell generation or scour-hole growth. However, De Serres et al. [57] found that the highest flows on the Bayonne-Berthier, cause the development of a small but noticeable scour-hole. A possible explanation for this is that the higher water depths weaken the effect of the bed discordance. There is, hence, no clear relationship between bed discordance and scour-hole.

Bed discordance at river confluences can also affect the development of other morphological features such as lateral bars. Where there is a significant step, it is known that the near-bed flow from the main channel passes under the tributary flow before being upwelled at the downstream corner [55,57,58,71]. This naturally provides a potential sediment transport path for main channel sediments to reach the downstream junction corner and form a lateral bar. Leite Ribeiro et al. [83] proposed that in the case of significant bed discordance, this process is facilitated by coarse sediment, which is passed to the post confluence channel from the tributary and joins this near-bed flow towards the downstream corner. Sukhodolov et al. found that flow at a discordant alluvial confluence with a velocity ratio larger than 2 exhibits jet-like features, thereby having important implications for morphodynamic processes [103].

In sum, bed discordance has an essential effect on the flow regime, sediment motion, and the resulting morphology in a confluence. Given the evidence that the effect of bed discordance varies with the river stage [57], it also provides a possible cause for confluence evolutions subjected to tidal and non-tidal flows. Changes to the overall discharge, river-runoff or tides, flowing through the

confluence in relation to bed discordance, require further explorations that will help the understandings of morpho-dynamics.

5. Conclusions

Confluence, as a natural component in river systems, controls the routing of flow and sediment and geomorphological stability. Existing research provides a good account of information about morpho-dynamics of the river junctions, especially the unidirectional (non-tidal) ones. In bi-directional flows, the shift of the dominant processes between run-off and tides featuring periodical changes in both magnitude and direction makes the confluence behaviors more complex. To date, limited research has been conducted for tidal confluences.

In the tidal and non-tidal environments, a thorough review of river confluences, in terms of flow, sediment, and morphology, has been summarized and discussed. Main conclusions include:

(1) There is a reciprocal adjustment of flow, sediment, and morphology at a confluence, and its behaviors differ greatly in the tidal and non-tidal environments. It is not reasonable that a river system, in terms of the three components, is studied in isolation, especially for its long-term behavior.

(2) Six notable hydraulic zones are identified for unidirectional confluences; of particular research interest is the separation zone and the shear layer. However, in tidal confluences, the flow patterns in terms of the conventional flow zone definitions are different. The flow zones always remain in transition and repeat in a tide cycle, showing four different arrangements of hydrodynamic features.

(3) Typical morphological features in the confluence, e.g., scour-hole, mid-channel bars, and bank attached bars, are investigated. Particularly, in the tidal and non-tidal environment, the relationship between scour-hole depth and confluence angle is revealed, showing a positively correlated feature.

(4) Turbulence and secondary circulation are enhanced with an increase in confluence angles with discharge and velocity ratios much greater or lower than one, and with the existence of bed discordance. In turn, this increased secondary flow also affects the morphology of the confluent areas.

All of the available research provides insights into the morpho-dynamics in tidal and non-tidal confluences. To comprehensively determine their behaviors is still challenging in the field of geomorphology, especially for the tidal cases. It is advisable to see extensive field measurement data and theoretical progress as foundations to help in understanding the sediment dynamics in the future. Some recommendations on future research prospects are put forward: (a) the effect of confluence angle (very acute/obtuse angles), tidal type (diurnal/ semi-diurnal), and bed discordance on near-surface flow features and morphological changes needs further exploration; (b)the study of 3D confluent flow structures during different tidal phases in a large river system is desired; (c) the scour-hole features, typically the morphology pattern, its presence, and evolution need extensive investigation.

Author Contributions: A.B., Q.X., and Y.Z. contributed equally to the writing of the manuscript. A.B. and Q.X. drafted the original manuscript, with modifications from Y.Z. The tables and figures were produced by A.B. and Q.X. The manuscript was revised by Q.X. and Y.Z., with assistance from A.B. All authors have read and agreed to the published version of the manuscript.

Funding: The authors were all supported by the Chinese Scholarship Council (CSC), and Q.X. was also funded by the Swedish StandUp for Energy project.

Acknowledgments: The authors would like to thank James Yang at the Royal Institute of Technology (KTH), T. Staffan Lundström at Luleå University of Technology (LTU), and Wenhong Dai at Hohai University (HHU) for their supervisions and comments that have improved the quality of the article. Q.X. thanks David R. Fuhrman at Denmark Technical University for the host and assistance during the visit as a guest researcher.

Conflicts of Interest: The authors declare no conflict of interest.

References

1. Taylor, E.H. Flow characteristics at rectangular open-channel junctions. *Trans. Am. Soc. Civ. Eng.* **1944**, *109*, 893–902.
2. Miller, J.P. *High Mountain Streams: Effects of Geology on Channel Characteristics and Bed Material*; State Bureau of Mines and Mineral Resources, New Mexico Institute of Mining and Technology, Socorro, New Mexico, 1958.
3. Mosley, M.P. An experimental study of channel confluences. *J. Geol.* **1976**, *84*, 535–562, doi:10.1086/628230.
4. Best, J.L. Flow Dynamics and Sediment Transport at River Channel Confluences. Ph.D. Thesis, University of London, London, UK, 1985.
5. Best, J.L. Sediment transport and bed morphology at river channel confluences. *Sedimentology* **1988**, *35*, 481–498, doi:10.1111/j.1365-3091.1988.tb00999.x.
6. Yuan, S.; Tang, H.; Xiao, Y.; Qiu, X.; Xia, Y. Water flow and sediment transport at open-channel confluences: An experimental study. *J. Hydraul. Res.* **2018**, *56*, 333–350, doi:10.1080/00221686.2017.1354932.
7. Dixon, S.J.; Smith, G.H.S.; Best, J.L.; Nicholas, A.P.; Bull, J.M.; Vardy, M.E.; Sarker, M.H.; Goodbred, S. The planform mobility of river channel confluences: Insights from analysis of remotely sensed imagery. *Earth-Sci. Rev.* **2018**, *176*, 1–18, doi:10.1016/j.earscirev.2017.09.009.
8. Umar, M.; Rhoads, B.L.; Greenberg, J.A. Use of multispectral satellite remote sensing to assess mixing of suspended sediment downstream of large river confluences. *J. Hyd.* **2018**, *556*, 325–338.
9. Lanzoni, S. Long-term evolution and morphodynamic equilibrium of tidal channels. *JGR* **2002**, *107*, doi:10.1029/2000jc000468.
10. Seminara, G.; Lanzoni, S.; Tambroni, N.; Toffolon, M. How long are tidal channels? *JFM* **2010**, *643*, 479–494, doi:10.1017/S0022112009992308.
11. Leeder, M.R. On the interactions between turbulent flow, sediment transport and bedform mechanics in channelized flows. In *Modern and Ancient Fluvial Systems*; Collinson, J.D., Lewin, J., Eds. Blackwell Scientific Publications, Oxford, UK, 1983; doi:10.1002/9781444303773.ch1.
12. Ashworth, P.J.; Ferguson, R.I. Interrelationships of channel processes, changes and sediments in a proglacial braided river. *Geogr. Ann. Ser. A Phys. Geogr.* **1986**, *68*, 361–371, doi:10.2307/521527.
13. Pittaluga, M.B.; Tambroni, N.; Canestrelli, A.; Slingerland, R.; Lanzoni, S.; Seminara, G. Where river and tide meet: The morphodynamic equilibrium of alluvial estuaries. *J. Geophys. Res. Earth Surf.* **2015**, *120*, 75–94, doi:10.1002/2014JF003233.
14. Xie, Q.; Yang, J.; Lundström, S.; Dai, W. Understanding morphodynamic changes of a tidal river confluence through field measurements and numerical modeling. *Water* **2018**, *10*, 1424–1432.
15. Zhou, Z.; Coco, G.; Townend, I.; Olabarrieta, M.; van der Wegen, M.; Gong, Z.; D'Alpaos, A.; Gao, S.; Jaffe, B.E.; Gelfenbaum, G., et al. Is "Morphodynamic Equilibrium" an oxymoron? *Earth-Sci. Rev.* **2017**, *165*, 257–267, doi:10.1016/j.earscirev.2016.12.002.
16. Wolfram, P.J.; Fringer, O.B.; Monsen, N.E.; Gleichauf, K.T.; Fong, D.A.; Monismith, S.G. Modeling intrajunction dispersion at a well-mixed tidal river junction. *J. Hydraul. Eng.* **2016**, *142*, 04016019, doi:10.1061/(ASCE)HY.1943-7900.0001108.
17. Gleichauf, K.; Wolfram, P.; Monsen, N.; Fringer, O.; Monismith, S. Dispersion mechanisms of a tidal river junction in the sacramento–san joaquin delta, california. *San Fr. Estuary Watershed Sci.* **2014**, *12*, 1–23, doi:10.15447/sfews.2014v12iss4art1.
18. Ginsberg, S.S.; Perillo, G.M.E. Deep-scour holes at tidal channel junctions, Bahia Blanca Estuary, Argentina. *Mar. Geol.* **1999**, *160*, 171–182, doi:10.1016/S0025-3227(99)00019-5.
19. Ginsberg, S.S.; Perillo, G.M.E. Characteristics of tidal channels in a mesotidal Estuary of Argentina. *J. Coast. Res.* **2004**, *20*, 489–497, doi:10.2112/1551-5036(2004)020[0489:COTCIA]2.0.CO;2.
20. Gomez, B.; Cui, Y.; Kettner, A.J.; Peacock, D.H.; Syvitski, J.P.M. Simulating changes to the sediment transport regime of the Waipaoa River, New Zealand, driven by climate change in the twenty-first century. *GPC* **2009**, *67*, 153–166, doi:10.1016/j.gloplacha.2009.02.002.
21. Ferrarin, C.; Madricardo, F.; Rizzetto, F.; Kiver, W.M.; Bellafiore, D.; Umgiesser, G.; Kruss, A.; Zaggia, L.; Foglini, F.; Ceregato, A., et al. Geomorphology of scour holes at tidal channel confluences. *J. Geophys. Res. Earth Surf.* **2018**, *123*, 1386–1406, doi:10.1029/2017JF004489.
22. Ashmore, P.E.; Ferguson, R.I.; Prestegaard, K.L.; Ashworth, P.J.; Paola, C. Secondary flow in anabranch confluences of a braided, gravel-bed stream. *Earth Surf. Process. Landf.* **1992**, *17*, 299–311, doi:10.1002/esp.3290170308.

23. Best, J.L.; Rhoads, B.L. *Sediment Transport, Bed Morphology and the Sedimentology of River Channel Confluences*; John Wiley & Sons, Ltd.: Chichester, UK, 2008; pp. 45–72, doi:10.1002/9780470760383.ch4.
24. Biswal, S.K.; Mohapatra, P.K.; Muralidhar, K. Flow separation at an open channel confluence. *ISH J. Hydraul. Eng.* **2010**, *16*, 89–98, doi:10.1080/09715010.2010.10515018.
25. Canelas, O.B.; Ferreira, R.M.L.; Guillén-Ludeña, S.; Alegria, F.C.; Cardoso, A.H. Three-dimensional flow structure at fixed 70° open-channel confluence with bed discordance. *J. Hydraul. Res.* **2019**, *58*, 434–446, doi:10.1080/00221686.2019.1596988.
26. Biron, P.M.; Robson, C.; Lapointe, M.F.; Gaskin, S.J. Comparing different methods of bed shear stress estimates in simple and complex flow fields. *Earth Surf. Process. Landf.* **2004**, *29*, 1403–1415, doi:10.1002/esp.1111.
27. Constantinescu, G.; Miyawaki, S.; Rhoads, B.; Sukhodolov, A.; Kirkil, G. Structure of turbulent flow at a river confluence with momentum and velocity ratios close to 1: Insight provided by an eddy-resolving numerical simulation. *Water Resour. Res.* **2011**, *47*, doi:10.1029/2010WR010018.
28. Dai, W.; Bilal, A.; Xie, Q.; Ahmad, I.; Joshi, I. Numerical modeling for hydrodynamics and near-surface flow patterns of a tidal confluence. *J. Coast. Res.* **2020**, *36*, 295–312, doi:10.2112/JCOASTRES-D-19-00058.1.
29. Xie, Q.; Yang, J.; Lundström, T.S. Field studies and 3D modelling of morphodynamics in a meandering river reach dominated by tides and suspended load. *Fluids* **2019**, *4*, 15.
30. Dordevic, D. Numerical study of 3D flow at right-angled confluences with and without upstream planform curvature. *J. Hydroinformatics* **2013**, *15*, 1073–1088, doi:10.2166/hydro.2012.150.
31. Bradbrook, K.F. Numerical, Field and Laboratory Studies of Three-Dimensional Flow Structures at River Channel Confluences. Ph.D. Thesis, University of Cambridge, Cambridge, UK, 1999.
32. Best, J.L. The morphology of river channel confluences. *Prog. Phys. Geogr.* **1986**, *10*, 157–174, doi:10.1177/030913338601000201.
33. Mackay, J.R. Lateral mixing of the Liard and Mackenzie rivers downstream from their confluence. *CaJES* **1970**, *7*, 111–124, doi:10.1139/e70-008.
34. Best, J.L.; Roy, A.G. Mixing-layer distortion at the confluence of channels of different depth. *Nature* **1991**, *350*, 411–413, doi:10.1038/350411a0.
35. Lane, S.N.; Parsons, D.R.; Best, J.L.; Orfeo, O.; Kostaschuk, R.A.; Hardy, R.J. Causes of rapid mixing at a junction of two large rivers: Río Paraná and Río Paraguay, Argentina. *J. Geophys. Res. Earth Surf.* **2008**, *113*, 1–16, doi:10.1029/2006JF000745.
36. Parsons, D.R.; Best, J.L.; Lane, S.N.; Kostaschuk, R.A.; Hardy, R.J.; Orfeo, O.; Amsler, M.L.; Szupiany, R.N. Large river channel confluences. In *River Confluences, Tributaries and the Fluvial Network*; Rice, S.P., Roy, A.G., Rhoads, B.L., Eds.; John Wiley & Sons: Chichester, UK, 2008; pp. 73–91.
37. Sukhodolov, A.N.; Schnauder, I.; Uijttewaal, W.S.J. Dynamics of shallow lateral shear layers: Experimental study in a river with a sandy bed. *Water Resour. Res.* **2010**, *46*, 1–18, doi:10.1029/2010WR009245.
38. Vermaas, D.A.; Uijttewaal, W.S.J.; Hoitink, A.J.F. Lateral transfer of streamwise momentum caused by a roughness transition across a shallow channel. *Water Resour. Res.* **2011**, *47*, 1–12, doi:10.1029/2010WR010138.
39. Guillén-Ludeña, S.; Franca, M.J.; Alegria, F.; Schleiss, A.J.; Cardoso, A.H. Hydromorphodynamic effects of the width ratio and local tributary widening on discordant confluences. *Geomorphology* **2017**, *293*, 289–304.
40. Uijttewaal, W.S.J.; Booij, R. Effects of shallowness on the development of free-surface mixing layers. *Phys. Fluids* **2000**, *12*, 392–402, doi:10.1063/1.870317.
41. Tang, H.; Zhang, H.; Yuan, S. Hydrodynamics and contaminant transport on a degraded bed at a 90-degree channel confluence. *Environ. Fluid Mech.* **2017**, *18*, 443–463, doi:10.1007/s10652-017-9562-8.
42. Biron, P.M.; Ramamurthy, A.S.; Han, S. Three-dimensional numerical modeling of mixing at river confluences. *J. Hydraul. Eng.* **2004**, *130*, 243–253, doi:10.1061/(ASCE)0733-9429(2004)130:3(243).
43. Bouchez, J.; Lajeunesse, E.; Gaillardet, J.; France-Lanord, C.; Dutra-Maia, P.; Maurice, L. Turbulent mixing in the Amazon River: The isotopic memory of confluences. *Eearth Planet. Sci. Lett.* **2010**, *290*, 37–43, doi:10.1016/j.epsl.2009.11.054.
44. Rhoads, B.L.; Kenworthy, S.T. Flow structure at an asymmetrical stream confluence. *Geomorphology* **1995**, *11*, 273–293, doi:10.1016/0169-555X(94)00069-4.
45. Biron, P.M.; Lane, S.N. *Modelling Hydraulics and Sediment Transport at River Confluences*; John Wiley & Sons, Ltd.: Chichester, UK, 2008; pp. 17–43, doi:10.1002/9780470760383.ch3.

46. Boyer, C.; Roy, A.G.; Best, J.L. Dynamics of a river channel confluence with discordant beds: Flow turbulence, bed load sediment transport, and bed morphology. *J. Geophys. Res. Earth Surf.* **2006**, *111*, 1–22.
47. Rhoads, B.L.; Sukhodolov, A.N. Lateral momentum flux and the spatial evolution of flow within a confluence mixing interface. *Water Resour. Res.* **2008**, *44*, 1–17, doi:10.1029/2007WR006634.
48. Rhoads, B.L.; Kenworthy, S.T. Time-averaged flow structure in the central region of a stream confluence. *Earth Surf. Process. Landf.* **1998**, *23*, 171–191.
49. Rhoads, B.L.; Sukhodolov, A.N. Spatial and temporal structure of shear layer turbulence at a stream confluence. *Water Resour. Res.* **2004**, *40*, 1–13, doi:10.1029/2003WR002811.
50. Rhoads, B.L.; Sukhodolov, A.N. Field investigation of three-dimensional flow structure at stream confluences: 1. Thermal mixing and time-averaged velocities. *Water Resour. Res.* **2001**, *37*, 2393–2410, doi:doi:10.1029/2001WR000316.
51. Biron, P.M.; Richer, A.; Kirkbride, A.D.; Roy, A.G.; Han, S. Spatial patterns of water surface topography at a river confluence. *Earth Surf. Process. Landf.* **2002**, *27*, 913–928, doi:doi:10.1002/esp.359.
52. Best, J.L.; Reid, I. Separation zone at open-channel junctions. *J. Hydraul. Eng.* **1984**, *110*, 1588–1594, doi:10.1061/(ASCE)0733-9429(1984)110:11(1588).
53. Huang, J.; Larry, J.W.; Yong, G.L. Three-dimensional numerical study of flows in open-channel junctions. *J. Hydraul. Eng.* **2002**, *128*, 268–280, doi:10.1061/(ASCE)0733-9429(2002)128:3(268).
54. Unde, M.G.; Dhakal, S. Sediment characteristics at river confluences: A case study of the Mula-Kas confluence, Maharashtra, India. *Prog. Phys. Geogr. Earth Environ.* **2009**, *33*, 208–223, doi:10.1177/0309133309338655.
55. Biron, P.M.; Roy, A.G.; Best, J.L.; Boyer, C.J. Bed morphology and sedimentology at the confluence of unequal depth channels. *Geomorphology* **1993**, *8*, 115–129, doi:10.1016/0169-555X(93)90032-W.
56. Bradbrook, K.F.; Lane, S.N.; Richards, K.S.; Biron, P.M.; Roy, A.G. Role of bed discordance at asymmetrical river confluences. *J. Hydraul. Eng.* **2001**, *127*, 351–368, doi:10.1061/(ASCE)0733-9429(2001)127:5(351).
57. De Serres, B.; Roy, A.G.; Biron, P.M.; Best, J.L. Three-dimensional structure of flow at a confluence of river channels with discordant beds. *Geomorphology* **1999**, *26*, 313–335, doi:10.1016/S0169-555X(98)00064-6.
58. Biron, P.; Best, J.L.; André, G.R. Effects of bed discordance on flow dynamics at open channel confluences. *J. Hydraul. Eng.* **1996**, *122*, 676–682, doi:10.1061/(ASCE)0733-9429(1996)122:12(676).
59. Rhoads, B.L.; Riley, J.D.; Mayer, D.R. Response of bed morphology and bed material texture to hydrological conditions at an asymmetrical stream confluence. *Geomorphology* **2009**, *109*, 161–173, doi:10.1016/j.geomorph.2009.02.029.
60. Szupiany, R.N.; Amsler, M.L.; Parsons, D.R.; Best, J.L. Morphology, flow structure, and suspended bed sediment transport at two large braid-bar confluences. *Water Resour. Res.* **2009**, *45*, 1–19, doi:10.1029/2008WR007428.
61. Wallis, E.; Nally, R.M.; Lake, P.S. A Bayesian analysis of physical habitat changes at tributary confluences in cobble-bed upland streams of the Acheron River basin, Australia. *Water Resour. Res.* **2008**, *44*, 1–10, doi:10.1029/2008WR006831.
62. Cushman-Roisin, B.; Constantinescu, G.S. Dynamical adjustment of two streams past their confluence. *J. Hydraul. Res.* **2019**, *2019*, 1–9, doi:10.1080/00221686.2019.1573765.
63. Benda, L. Confluence environments at the scale of river networks. In *River Confluences, Tributaries and the Fluvial Network*; Rice, S.P., Roy, A.G., Rhoads, B.L., Eds.; John Wiley & Sons: Chichester, UK, 2008; p. 466, doi:10.1002/9780470760383.ch13.
64. Ferguson, R.; Hoey, T. *Effects of Tributaries on Main-Channel Geomorphology*; John Wiley & Sons, Ltd.: Chichester, UK, 2008; pp. 183–208, doi:10.1002/9780470760383.ch10.
65. Rice, S.P. Which tributaries disrupt downstream fining along gravel-bed rivers? *Geomorphology* **1998**, *22*, 39–56, doi:10.1016/S0169-555X(97)00052-4.
66. Rice, S.P.; Kiffney, P.; Greene, C.; Pess, G.R. *The Ecological Importance of Tributaries and Confluences*; John Wiley & Sons, Ltd.: Chichester, UK, 2008; pp. 209–242, doi:10.1002/9780470760383.ch11.
67. Rice, S.P.; Rhoads, B.L.; Roy, A.G. *Introduction: River Confluences, Tributaries and the Fluvial Network*; John Wiley & Sons, Ltd.: Chichester, UK, 2008; pp. 1–9, doi:10.1002/9780470760383.ch1.
68. Benda, L.; Veldhuisen, C.; Black, J. Debris flows as agents of morphological heterogeneity at low-order confluences, Olympic Mountains, Washington. *GSAMB* **2003**, *115*, 1110–1121, doi:10.11130/B25265.1.

69. Curtis, K.E.; Renshaw, C.E.; Magilligan, F.J.; Dade, W.B. Temporal and spatial scales of geomorphic adjustments to reduced competency following flow regulation in bedload-dominated systems. *Geomorphology* **2010**, *118*, 116–129.
70. Musselman, Z.A. The localized role of base level lowering on channel adjustment of tributary streams in the Trinity River basin downstream of Livingston Dam, Texas, USA. *Geomorphology* **2011**, *128*, 42–56, doi:10.1016/j.geomorph.2010.12.021.
71. Biron, P.; Roy, A.G.; Best, J.L. Turbulent flow structure at concordant and discordant open-channel confluences. *Exp. Fluids* **1996**, *21*, 437–446, doi:10.1007/BF00189046.
72. Bridge, J.S.; Gabel, S.L. Flow and sediment dynamics in a low sinuosity, braided river: Calamus River, Nebraska Sandhills. *Sedimentology* **1992**, *39*, 125–142, doi:10.1111/j.1365-3091.1992.tb01026.x.
73. Bradbrook, K.F.; Biron, P.M.; Lane, S.N.; Richards, K.S.; Roy, A.G. Investigation of controls on secondary circulation in a simple confluence geometry using a three-dimensional numerical model. *HyPr Hydrol. Process.* **1998**, *12*, 1371–1396, doi:10.1002/(SICI)1099-1085(19980630)12:8<1371::AID-HYP620>3.0.CO;2-C.
74. Dai, W.; Bilal, A.; Xie, Q.; Zhai, Y. Numerical simulation of a deep-scour hole in a tidal river confluence using Delft 3D. In Proceedings the 37th IAHR World Congress, Kuala Lumpur, Malaysia, 13–18 August 2017; pp. 633–638.
75. Gaucherel, C.; Frelat, R.; Salomon, L.; Rouy, B.; Pandey, N.; Cudennec, C. Regional watershed characterization and classification with river network analyses. *Earth Surf. Process. Landf.* **2017**, *42*, 2068–2081, doi:10.1002/esp.4172.
76. Jung, K.; Marpu, P.R.; Ouarda, T. Impact of river network type on the time of concentration. *Arab. J. Geosci.* **2017**, *10*, 1–17, doi:10.1007/s12517-017-3323-3.
77. Seo, Y.; Schmidt, A.R. Application of Gibbs' model to urban drainage networks: A case study in southwestern Chicago, USA. *Hydrol. Process.* **2014**, *28*, 1148–1158, doi:10.1002/hyp.9657.
78. Ashmore, P.E.; Parker, G. Confluence scour in coarse braided streams. *Water Resour. Res.* **1983**, *19*, 392–402, doi:10.1029/WR019i002p00392.
79. Best, J.L. Flow dynamics at river channel confluences: Implications for sediment transport and bed morphology. In *Recent Developments in Fluvial Sedimentology*; Ethridge, F.G., Flores, R.M., Harvey, M.D., Eds.; SEPM Society for Sedimentary Geology: Tulsa, OK, USA, 1987; Volume 39, p. 371.
80. Xie, Q. Field Measurements and Numerical Simulations of Sediment Transport in a Tidal River. Licentiate Thesis, Luleå University of Technology, Luleå, Sweden, 2019.
81. Guillén-Ludeña, S. *Hydro-Morphodynamics of Open-Channel Confluences with Low Discharge Ratio and Dominant Tributary Sediment Supply*; EPFL: Lausanne, Switzerland, 2015.
82. Guillen-Ludena, S.; Franca, M.J.; Cardoso, A.H.; Schleiss, A.J. Evolution of the hydromorphodynamics of mountain river confluences for varying discharge ratios and junction angles. *Geomorphology* **2016**, *255*, 1–15.
83. Leite Ribeiro, M.; Blanckaert, K.; Roy, A.G.; Schleiss, A.J. Flow and sediment dynamics in channel confluences. *J. Geophys. Res. Earth Surf.* **2012**, *117*, 1–19, doi:10.1029/2011JF002171.
84. Sukhodolov, A.N.; Rhoads, B.L. Field investigation of three-dimensional flow structure at stream confluences: 2. Turbulence. *Water Resour. Res.* **2001**, *37*, 2411–2424, doi:10.1029/2001wr000317.
85. Ashmore, P.E.; Gardner, J.T. Unconfined Confluences in Braided Rivers. John Wiley & Sons, Ltd.: Chichester, UK, 2008; 10.1002/9780470760383.ch7pp. 119-147.
86. Roy, A.G.; Bergeron, N. Flow and particle paths at a natural river confluence with coarse bed material. *Geomorphology* **1990**, *3*, 99–112, doi:10.1016/0169-555X(90)90039-S.
87. Tancock, M.J. The Dynamics of Upland River Confluences. Ph.D. Thesis, Durham University, Durham, UK, 2014.
88. Bertoldi, W.; Zanoni, W.L.; Tubino, M. Assessment of morphological changes induced by flow and flood pulses in a gravel bed braided river: The Tagliamento River (Italy). *Geomorphology* **2010**, *114*, 348–360.
89. Lancaster, S.T.; Underwood, E.F.; Frueh, W.T. Sediment reservoirs at mountain stream confluences: Dynamics and effects of tributaries dominated by debris-flow and fluvial processes. *GSAMB* **2010**, *122*, 1775–1786.
90. Kjerfve, B.; Shao, C.-C.; Stapor, F.W. Formation of deep scour holes at the junction of tidal creeks: An hypothesis. *Mar. Geol.* **1979**, *33*, M9–M14, doi:10.1016/0025-3227(79)90126-9.
91. Sambrook-Smith, G.H.; Ashworth, P.J.; Best, J.L.; Woodward, J.; Simpson, C.J. The morphology and facies of sandy braided rivers: Some considerations of scale invariance. In *Fluvial Sedimentology VII*; Blum, M.D.,

Marriott, S.B., Leclair, S.F., Eds.; Wiley-Blackwell, New Jersey, NJ, US: 2005; pp. 145–158, doi:10.1002/9781444304350.ch9.

92. Orfeo, O.; Parsons, D.R.; Best, J.L.; Lane, S.N.; Hardy, R.J.; Kostaschuk, R.A.; Szupiany, R.N.; Amsler, M.L. Morphology and flow structures in a large confluence-diffluence. In Proceedings of the International Conference on Fluvial Hydraulics, Lisbon, Purtagal, 6–8 September 2006; pp. 1277–1282.
93. Bradbrook, K.F.; Lane, S.N.; Richards, K.S. Numerical simulation of three-dimensional, time-averaged flow structure at river channel confluences. *Water Resour. Res.* **2000**, *36*, 2731–2746, doi:10.1029/2000WR900011.
94. Bradbrook, K.F.; Lane, S.N.; Richards, K.S.; Biron, P.M.; Roy, A.G. Large Eddy Simulation of periodic flow characteristics at river channel confluences. *J. Hydraul. Res.* **2000**, *38*, 207–215, doi:10.1080/00221680009498338.
95. Penna, N.; De Marchis, M.; Canelas, O.; Napoli, E.; Cardoso, A.; Gaudio, R. Effect of the junction angle on turbulent flow at a hydraulic confluence. *Water* **2018**, *10*, 1–23.
96. Riley, J.D.; Rhoads, B.L.; Parsons, D.R.; Johnson, K.K. Influence of junction angle on three-dimensional flow structure and bed morphology at confluent meander bends during different hydrological conditions. *Earth Surf. Process. Landf.* **2015**, *40*, 252–271, doi:10.1002/esp.3624.
97. Bryan, R.B.; Kuhn, N.J. Hydraulic conditions in experimental rill confluences and scour in erodible soils. *Water Resour. Res.* **2002**, *38*, 1–13.
98. Constantinescu, G.; Miyawaki, S.; Rhoads, B.; Sukhodolov, A. Numerical analysis of the effect of momentum ratio on the dynamics and sediment-entrainment capacity of coherent flow structures at a stream confluence. *J. Geophys. Res. Earth Surf.* **2012**, *117*, 1–21, doi:10.1029/2012JF002452.
99. Thompson, C.J.; Croke, J.C.; Purvis-Smith, D. Floodplain sediment disconnectivity at a tributary junction and valley constriction site in the Fitzroy River basin, Queensland, Australia. *Geomorphology* **2011**, *125*, 293–304.
100. Schindfessel, L.; Creelle, S.; De Mulder, T. Flow patterns in an open channel confluence with increasingly dominant tributary inflow. *Water* **2015**, *7*, 4724–4751.
101. Gaudet, J.M.; Roy, A.G. Effect of bed morphology on flow mixing length at river confluences. *Nature* **1995**, *373*, 138–139, doi:10.1038/373138a0.
102. Ludeña, S.G.; Cheng, Z.; Constantinescu, G.; Franca, M.J. Hydrodynamics of mountain-river confluences and its relationship to sediment transport. *J. Geophys. Res. Earth Surf.* **2017**, *122*, 901–924, doi:10.1002/2016JF004122.
103. Sukhodolov, A.N.; Krick, J.; Sukhodolova, T.A.; Cheng, Z.; Rhoads, B.L.; Constantinescu, G.S. Turbulent flow structure at a discordant river confluence: Asymmetric jet dynamics with implications for channel morphology. *J. Geophys. Res. Earth Surf.* **2017**, *122*, 1278–1293, doi:10.1002/2016jf004126.